Simultaneous Supralinear Line-Narrowing and Sensitivity Enhancement at High Fields in Magic Angle Spinning NMR of Spin-1/2 Nuclei in Solids

Riqiang Fu,*,[†] Ozge Gunaydin-Sen,[‡] and Naresh S. Dalal*,[‡]

National High Magnetic Field Laboratory and Department of Chemistry and Biochemistry, Florida State University, Tallahassee, Florida 32310

Advantages of very high fields in nuclear magnetic resonance (NMR) include the improved sensitivity, increased chemical shift dispersion, reduced second-order quadrupolar interactions, improved relaxation properties, and many others.[1] Such advantages have been well demonstrated for liquids[1−3] and for aligned samples.[4] For quadrupolar nuclei in solids, the line-narrowing effects are at least quadratic with the static magnetic field, B_0, because of the combination of the chemical shift dispersion and the reduction of the second-order line broadening at high fields.[5,6] However, the situation is less clear for spin-1/2 nuclei in solids, related in part to bulk magnetic susceptibility line-broadening effects,[7] which also scale with B_0. One technique that is proving highly useful for minimizing the magnetic susceptibility effects in solids is magic angle spinning (MAS) of a single crystal,[8] especially as applied to the study of solid−solid phase transitions in which the resolution enhancement is crucial.[9] It is thus of interest to examine if high fields do provide an improvement in resolution in MAS NMR measurements of spin-1/2 nuclei, using the highest available ultra-wide bore 900 MHz NMR spectrometer, currently operating at 21.1 T.[10]

Enhanced by cross polarization (CP) from protons, the ^{15}N CP/MAS NMR spectra of a ^{15}N-labeled $NH_4H_2AsO_4$ (henceforth, ADA) single crystal, an interesting antiferroelectric material,[11] were recorded at different static fields (7.0, 14.1, and 21.1 T), as shown in Figure 1. A small piece of ADA single crystal was packed in a 4-mm MAS rotor and used for NMR measurements on 300 and 600 MHz, while a slightly smaller piece was packed in a 3.2-mm MAS rotor for the measurements on 900 MHz. In order to fairly compare their respective ^{15}N line width at different static fields, the field shimming was performed prior to the ^{15}N measurements through minimizing the ^{13}C line width at half-height for the NMR resonances of natural abundance adamantane under high-power ^1H decoupling. Clearly, as listed in Table 1, the observed line width, Δv^*, of the ^{15}N ADA resonance greatly decreases from 0.260 to 0.071 ppm with the increase of the static fields from 300 to 900 MHz; that is, the spectral resolution improved by 366%. It is worth noting that the resolution enhancement is not linearly proportional to the magnetic field strength. From 300 to 600 MHz, the resolution is improved by 260%, while just by 140% from 600 to 900 MHz.

In order to understand the mechanism underlying the resolution enhancement, we measured the T_2 values at the various fields. The T_2 measurements were carried out using the standard spin−echo sequence in which a π pulse is placed in the middle of the ^{15}N spin−echo period, τ, to refocus the ^{15}N magnetization generated by CP. The ^1H decoupling during the evolution and acquisition periods was achieved by the efficient TPPM sequence.[12] Figure 2 shows the plots of the signal intensities versus the spin−echo time τ measured on the 300 and 900 MHz NMR spectrometers.
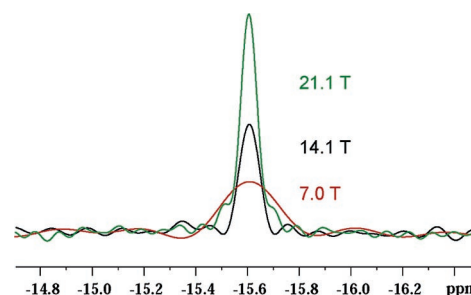
Figure 1. Field dependence of ^{15}N CP/MAS spectra of an ADA single crystal at 300 K at a spinning rate of 2.5 kHz, recorded on Bruker DMX300 (red), DRX600 (black), and the ultra-wide bore 900 NMR spectrometer (green), referenced to ^{15}N isotropy of powdered valine at 0 ppm. The signals were normalized to 32 scans. No line broadening was applied in these spectra.

Table 1. Resolution and Sensitivity Enhancement Factors of ^{15}N CP/MAS Signals for $NH_4H_2AsO_4$ at Various Static Fields

field (T)	Δv^* (ppm)	T_2 (ms)	$\Delta v = 1/\pi T_2$ (ppm)	(Hz)	S/N (obs)	S/N observed over $(B_0)^{3/2}$
7.0	0.260	138	0.077	2.31	1	1
14.1	0.100	160	0.033	1.98	4.44	1.6
21.1	0.071	163	0.022	1.95	18.22	2.7
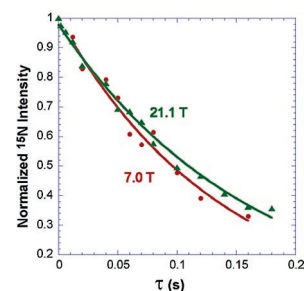


Figure 2. Normalized ^{15}N signal intensities of ADA as a function of spin−echo time τ, recorded from 300 (red) and 900 (green) MHz. Monoexponential fittings yield the transverse relaxation times of 138 and 163 ms for 300 and 900 MHz, respectively.

Apparently, the ^{15}N signal intensities decay monoexponentially as a function of τ, yielding transverse relaxation times T_2 of 138 and 163 ms for 300 and 900 MHz, respectively. These relaxation times translate into natural line widths of 2.31 and 1.95 Hz, which are generally smaller than the observed ones owing to the refocusing of shift distributions (e.g., B_0 inhomogeneity) in the T_2 measurements.[13] Table 1 lists the T_2 values measured at different fields and their respective natural line widths. As can be seen from Table 1, the natural line width decreases by 14% from 300 to 600 MHz while remains almost constant from 600 to 900 MHz. However, by taking into account the chemical shift dispersion at different fields, the spectral resolution enhancement improves by 233% from

[†] National High Magnetic Field Laboratory.
[‡] Department of Chemistry and Biochemistry.
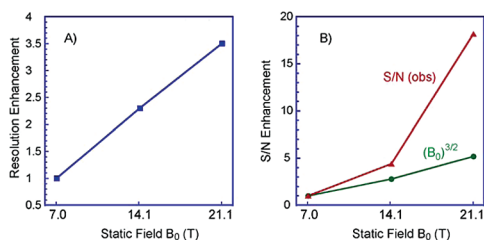
Figure 3. Resolution (A) and sensitivity (B) enhancement at various static fields B_0 after normalizing to the same number of scans.

300 to 600 MHz and 150% from 600 to 900 MHz, which is similar to the observed line widths (cf. Figure 1).

For relaxation mechanisms induced by spin interactions, the line width $\Delta\nu$ is proportional to the spectral densities, SDs.[14] As an example, for dipolar interactions, SDs can be rationalized by

$$\text{SD} = 3\tau_C + \frac{5\tau_C}{1 + \omega_0^2\tau_C^2} + \frac{2\tau_C}{1 + 4\omega_0^2\tau_C^2} \quad (1)$$

where ω_0 is the Lamor frequency and τ_C characterizes the lattice motion. For the extremely fast (i.e., $\omega_0\tau_C \ll 1$) and extremely slow (i.e., $\omega_0\tau_C \gg 1$) motions, the SDs are independent of B_0. However, for $\omega_0\tau_C \sim 1$, the SDs greatly depend on B_0 (see the Supporting Information). Although the SDs steadily increase as the motion slows down, for any given correlation time τ_C, higher static fields always give rise to smaller SDs, thus resulting in narrower line widths (or longer T_2 values). Such an increase in T_2 values at high fields was observed in solution NMR.[2] It is found that the most pronounced high field line-narrowing effect occurs at $\tau_C \sim 10^{-8}$ s. However, this field dependence of the line width is much more difficult to predict in solids in the presence of other significant line-broadening effects, such as bulk magnetic susceptibilities and chemical shift anisotropies at high fields.[7]

This high field line-narrowing effect not only results in spectral resolution enhancement but also leads to an improvement of the sensitivity beyond what is expected from the $(B_0)^{3/2}$ effect. The signal-to-noise ratios (S/N) measured from the spectra in Figure 1 were 9, 20, and 41 for 300, 600, and 900 MHz, respectively. Figure 3 shows the S/N and resolution enhancement versus B_0. Detailed analyses of the measured S/N (as documented in the Supporting Information) estimate an extra enhancement of a factor of 1.6 and 2.7 by going from 7.0 to 14.1 and to 21.1 T.

The enhanced resolution and sensitivity at 900 MHz enabled us to study the temperature dependence of the ^{15}N isotropic chemical shift variation through the antiferroelectric phase transition of ADA at 215 K. This study was undertaken to understand the role of the NH_4^+ ion in the transition mechanism since the substitution of NH_4^+ ion in place of K^+ in KH_2AsO_4 switches the latter compound from a ferroelectric to an antiferroelectric one.[15] Figure 4 shows the ^{15}N CP/MAS spectra recorded at 900 MHz in the close vicinity of the phase transition at $T_N \sim 215$ K. As the temperature approaches T_N, the paraelectric phase steadily disappears while the antiferro-electric phase gradually merges. The two phases, whose ^{15}N isotropic chemical shifts are just 0.3 ppm apart, coexist within 1.5 K. Such a small isotropic chemical shift difference can be hardly identified at lower fields. The sharp change in the isotropic chemical shift, δ_{iso}, at T_N implies that the NH_4^+ group takes part in the charge renormalization at the phase transition, and thus it is not just a spectator ion. Earlier theories of the ferroelectric (or antiferroelectric) behavior of this family of compounds have stressed the order–disorder role of the O–H···O protons in the transition mechanism. Specifically, the observation of the anomaly in δ_{iso} implies that
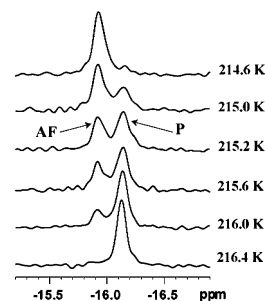
Figure 4. Temperature dependence of the ^{15}N CP/MAS NMR spectra of ADA in the close vicinity of the antiferroelectric phase transition recorded on the ultra-wide bore 900 MHz NMR spectrometer. The peaks corresponding to the paraelectric and antiferroelectric phases are labeled by P and AF, respectively.

the transition has a displacive character since δ_{iso} is invariant to any translational or rotational symmetry change (i.e., order–disorder effects). This aspect has not been appreciated in any earlier theory of transition in ADA and related antiferroelectrics.[8,9,15]

In summary, we have demonstrated that, for ^{15}N CP/MAS NMR experiments, both the spectral resolution and sensitivity improve significantly at higher static fields. The resolution enhancement seems to have its origin in the T_2 increase at higher fields. The enhanced resolution and sensitivity have enabled us to probe the nature of the antiferroelectric transition in ADA to a depth not possible at lower fields. These findings should open up new areas of investigations in NMR spectroscopy of solids, as well as its applications to new phenomenon in materials science.

Supporting Information Available: Material and experimental details, field dependence of SDs, S/N analyses, and complete ref 10. This material is available free of charge via the Internet at http://pubs.acs.org.

References

(1) Freeman, R.; Bobert, J.-B. *NMR, Basic Principles and Progress*; Springer-Verlag: Berlin, 1991; Vol. 25.
(2) Meersman, T.; Schwager, M.; Varma, V.; Bodenhausen, G. *J. Magn. Reson. Ser. A* **1996**, *119*, 275–279.
(3) Pervushin, K.; Riek, R.; Wider, G.; Wuthrich, K. *Proc. Natl. Acad. Sci. U.S.A.* **1997**, *94*, 12366–12371.
(4) Fu, R.; Cross, T. A. *Annu. Rev. Biophys. Biomol. Struct.* **1999**, *28*, 235–268.
(5) Gan, Z.; Gor'kov, P. L.; Cross, T. A.; Samoson, A.; Massiot, D. *J. Am. Chem. Soc.* **2002**, *124*, 5634–6535.
(6) Luga, D.; Morais, C.; Gan, Z.; Neuville, D. R.; Cormier, L.; Massiot, D. *J. Am. Chem. Soc.* **2005**, *127*, 11540–11541.
(7) VanderHart, D. L.; Earl, W. L.; Garroway, A. N. *J. Magn. Reson.* **1981**, *44*, 361–401.
(8) Dalal, N.; Klymachyov, A.; Bussman-Holder, A. *Phys. Rev. Lett.* **1998**, *81*, 5924–5927.
(9) Dalal, N. S.; Gunaydin-Sen, O.; Fu, R.; Achey, R.; Pierce, K. L. *Ferroelectrics* **2006**, *337*, 3–12.
(10) Fu, R.; et al. *J. Magn. Reson.* **2005**, *177*, 1–8.
(11) Gunaydin-Sen, O.; Fu, R.; Achey, R.; Dalal, N. S. *Ferroelectrics* **2006**, *337*, 153–160.
(12) Bennett, A. E.; Rienstra, C. M.; Auger, M.; Lakshmi, K. V.; Griffin, R. G. *J. Chem. Phys.* **1995**, *103*, 6951–6958.
(13) Paepe, G. D.; Giraud, N.; Lesage, A.; Hodgkinson, P.; Boeckmann, A.; Emsley, L. *J. Am. Chem. Soc.* **2003**, *125*, 13938–13939.
(14) Mehring, M. *Principles of High Resolution NMR in Solids*; 2nd ed.; Springer-Verlag: New York, 1983.
(15) Lines, M. E.; Glass, A. M. *Principles and Applications of Ferroelectrics and Related Materials*; Clarendon Press: Oxford, UK, 1977.

JA067179J